

Flexible color segmentation of biological images with the R package **recolorize**

Hannah I. Weller¹, Steven M. Van Belleghem², Anna E. Hiller³, and
Nathan P. Lord⁴

¹*Department of Ecology, Evolution, and Organismal Biology, Brown University, Providence,
RI, USA*

²*Department of Biology, University of Puerto Rico, Rio Piedras, Puerto Rico*

³*Museum of Natural Science and Department of Biological Sciences, Louisiana State
University, Baton Rouge, LA, USA*

⁴*Department of Entomology, Louisiana State University Agricultural Center, Baton Rouge,
LA, USA*

Abstract

Color is an important source of biological information in fields ranging from disease ecology to sexual selection. Despite its importance, most metrics for color are restricted to point measurements. Methods for moving beyond point measurements rely on color maps, where every pixel in an image is assigned to one of a set of discrete color classes (color segmentation). Manual methods for color segmentation are slow and subjective, while existing automated methods often fail due to

biological variation in pattern, technical variation in images, and poor scalability for batch clustering. As a result, color segmentation is the common bottleneck step for a majority of existing downstream analyses. Here we present **recolorize**, an R package for color segmentation that succeeds in many cases where existing methods fail. **Recolorize** has three major components: (1) an effective two-part clustering algorithm where color distributions are binned and combined according to perceived similarity in a frequency-independent manner; (2) a toolkit for minor manual adjustments to automatic output where needed; and (3) flexible export options. This paper illustrates how to use **recolorize** and compares it to existing methods, including examples where we segment formerly intractable images, and demonstrates the downstream use of methods that rely on color maps.

1 Introduction

2 Color is an important source of biological variation, and is an important trait in a wide
3 range of biological questions, ranging from sexual selection, camouflage, and animal com-
4 munication, to thermal physiology, disease ecology, development, and genetics (Bekker
5 et al., 1837; Bates, 1863; Poulton, 1890; Orteu and Jiggins, 2020; Hooper et al., 2020;
6 Van Belleghem et al., 2020). Despite their obvious importance in biology (e.g., signal
7 function, taxon identification, color production and variation), there is little consensus
8 about how to quantify and compare color patterns, even though this is a necessary first
9 step in testing most questions about them. Contrast this with, for example, geometric
10 morphometrics, a family of methods for quantifying variation in biological shape (Book-
11 stein, 1996). Researchers have reached a general consensus about how to quantify and

12 compare morphology (Klingenberg, 2011; Adams and Otárola-Castillo, 2013; Olsen and
13 Westneat, 2015). This consensus, coupled with the availability of a handful of software
14 tools for easily digitizing specimens, has led to a marked increase in both the number
15 of studies that use geometric morphometrics and the insights resulting from this work
16 (Polly et al., 2013; Adams et al., 2004; Lawing and Polly, 2010). There is no such set of
17 consensus methods for measuring variation in biological color.

18 Partly, lack of consensus is inevitable—color patterns are multidimensional and receiver-
19 dependent, so variation can come from a wide range of biological and technical sources
20 (this true to some extent for morphology, but at least this variation all exists in the same
21 three dimensions). Individual organisms might vary in the location, arrangement, and
22 intensity of their color pattern elements; the optical physical properties of those patterns
23 (pigmentary or structural); and the surface topology and 3D morphology of the organism
24 itself. Even if these sources of variation are well-defined, the ways in which we detect and
25 record this information can introduce noise and error.

26 Color pattern data is usually measured from images captured through digital sensors
27 constructed from human-centric visual system sensitivities, which can (and do) vary from
28 camera to camera. The colors reflected by a surface also depend on the available light,
29 whether natural or artificial, which varies in emission output, intensity, and direction,
30 all of which will affect how light reflects off of a given surface (with its own material
31 properties) (Johnsen, 2012). Given these constraints, it is not surprising that universal
32 methods for measuring color patterns in a consistent and repeatable way have remained
33 elusive. How do we meaningfully measure the difference between organisms that may not
34 have homologous color pattern elements? What if the images were taken with different

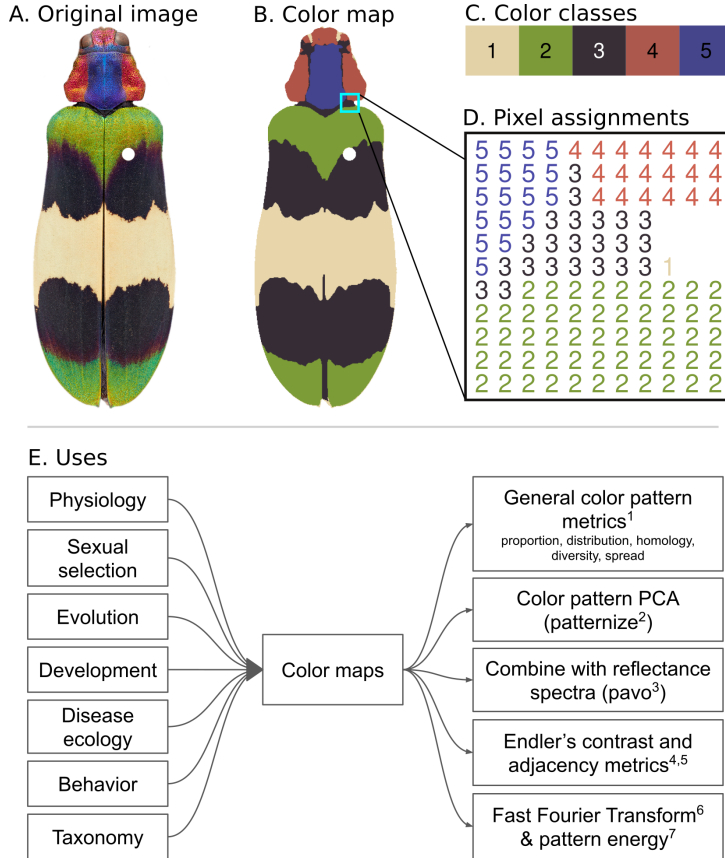


Figure 1: Color map example made with `recolorize`. A: Original image of a beetle, *Chrysochroa corbetti*. Limbs, antennae, and insect pin have all been masked. B: Color map, where each pixel has been assigned to one of five color classes. C: The five color classes displayed as a color palette; in this case the displayed colors of the palette (the color centers) represent the average red-green-blue (RGB) color of all pixels assigned to that class. D: A representative section of the color map as a numeric matrix: each pixel is assigned to a color class, so that we can refer to the entirety of color patch 2 by indexing all values of the color map equal to 2, which is associated with a particular color (in this case, green). E: Color maps are a major bottleneck step of color pattern quantification. The boxes on the left list some fields for which color pattern is an important trait; on the right are commonly used metrics or methods for quantifying color pattern, all of which require color maps as a starting point. Original image: Nathan P. Lord. Citations: 1. Chan et al. (2019); 2. Van Belleghem et al. (2018); 3. Maia et al. (2019); 4. Endler (2012); 5. Endler et al. (2018); 6. Mason et al. (2021); 7. van den Berg et al. (2020).

35 lighting conditions and cameras? What do we compare? How much can we reduce
36 this dimensionality and still retain the relevant variation—assuming we even know what
37 constitutes relevant variation?

38 Plenty of available methods exist for measuring particular aspects of color patterns,
39 but most of these are specific to a system or question. Researchers often have no choice
40 but to build a new method specific to their problem (Caves and Johnsen, 2018; Valcu and
41 Dale, 2014; Gawryszewski, 2018; Chan et al., 2019; van den Berg et al., 2020; Troscianko
42 et al., 2017; Yang et al., 2016; Van Belleghem et al., 2018; Maia et al., 2019; Weller
43 and Westneat, 2019; Hooper et al., 2020; Valvo et al., 2021; Endler et al., 2018; Endler,
44 2012; Ezray et al., 2019). This sets an unreasonably high barrier to entry for measuring
45 color patterns: developing methods is time-consuming and measurements are difficult to
46 compare.

47 Some of the most frequently used and promising methods for quantifying color pat-
48 tern variation are also the most flexible, in that they can be applied to a wide variety
49 of organisms and pattern types. Well-known examples include Endler’s adjacency and
50 boundary strength metrics (Endler, 2012; Endler et al., 2018), which emphasize contrast
51 between adjacent color patches; the `patternize` package (Van Belleghem et al., 2018),
52 which quantifies color pattern variation essentially using a sampling grid); the `micaTool-`
53 box suite of tools for multispectral image analysis (van den Berg et al., 2020); and the
54 matching of spatial image data with spectral reflectance data in the `pavo` package (Maia
55 et al., 2019). Most of these metrics require first clustering the image into discrete color
56 patches (making “color maps”) and then measuring how various aspects of these patches
57 vary across images (Fig. 1). Essentially, they start from the simplifying assumption that

58 a color pattern can be discretized into regions of uniform color, and then compare the
59 shape and color of those regions in some biologically relevant way.

60 Generating color maps from digital images—in a reproducible and efficient way—has
61 proven to be the bottleneck step for these methods, especially across sets of images

62 (Fig. 1E). Image segmentation in general is a notoriously complex problem, compounded
63 here by the fact that the number and boundaries of color patches are often ambiguous;

64 there isn't necessarily a 'correct' answer, just one appropriate to the biological question.

65 An image without some kind of segmentation, however, is little more than a pile of
66 pixels; segmentation provides labels to groups of pixels so that we can refer to (and

67 measure) particular regions. Researchers typically choose between automated methods,
68 which require little or no user input but are difficult to modify when they do not work

69 well, and manual segmentation, which is typically slow and subjective (Hooper et al.,
70 2020).

71 The most widely used automated method is k-means clustering (Hartigan and Wong,

72 1979), which has been implemented in several R packages for color pattern analysis
73 (Weller and Westneat, 2019; Van Belleghem et al., 2018; Maia et al., 2019), making it

74 more accessible than other approaches. Users specify only the expected number of color
75 classes, and the k-means algorithm attempts to find the set of color classes that minimize

76 within-cluster variances. While this is a relatively intuitive and flexible approach in
77 theory, in practice k-means clustering suffers from a number of issues:

- 78 1. In trying to minimize variances, k-means tends to over-cluster large color patches
79 and fails to differentiate small, colorful patches, meaning it often misses details and
80 is highly sensitive to shadows, 3D contours, texture, and specular reflections (all

81 frequent features of organism photographs) (Fig. 2A-B).

82 2. Users can't compare images that were taken from different sources or under differ-
83 ent lighting conditions, because they can produce very different color distributions

84 (Fig. 2C) that k-means clustering can't correct for.

85 3. Users have to specify the number of color classes, which is subjective, and for
86 comparative datasets may not be the same for all species (Fig. 2D).

87 4. The implementation of the algorithm is usually heuristic, not deterministic. The
88 same image will result in different color clusters depending on the run, and the
89 color classes themselves are returned in an arbitrary order. This makes it difficult
90 to perform batch processing when we want to map a set of images to the same set of
91 colors, because yellow might be color 1 in our first image and color 2 in our second
92 image (Fig. 2E), and the colors will be in a new random order every time we rerun
93 the analysis unless users set a particular seed at the start of a clustering session.

94 There are other methods for performing color segmentation, but they share many of

95 the same weaknesses as k-means or are otherwise too limited in scope to be as easily

96 generalized to a range of problems. Edge detection methods (e.g. watershedding, Otsu
97 algorithm, Canny operator) use spatial information, which can resolve glare and noise

98 to some extent, but only work well for segmenting color patches with sharp boundaries

99 and often treat textures like scales as edges. The receptor-noise limited (RNL) clustering

100 implemented in the Quantitative Color Pattern Analysis toolbox for ImageJ ([van den](#)

101 [Berg et al., 2020](#)), which uses properties of the visual system to segment colors based on

102 perceived color differences, works well under specific assumptions. However, it addresses

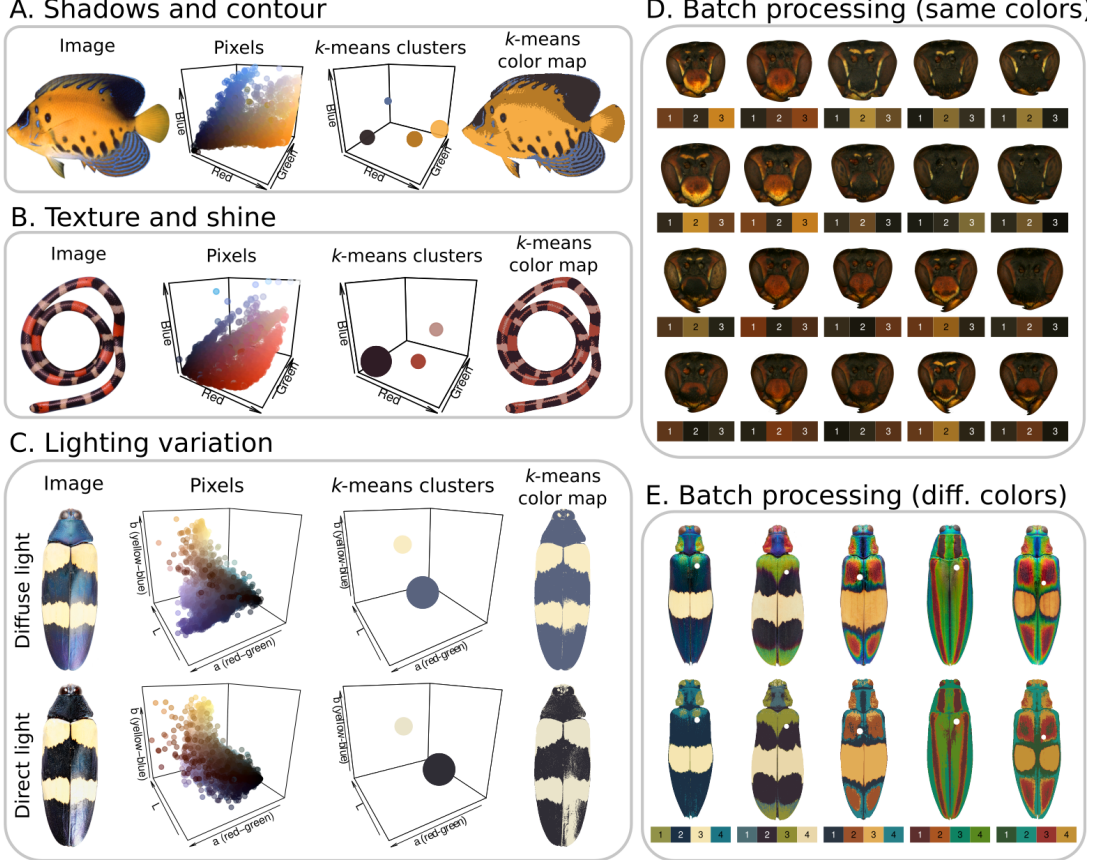


Figure 2: Examples of images and image sets for which k-means clustering is inadequate for color segmentation. A: This angelfish (*Pygoplites diacanthus*) has four color classes: yellow, black, blue, and white. K-means achieves lower within-cluster variances by assigning a light and dark yellow color center when we fit $n = 4$ centers. B: A coral snake (*Micrurus* sp.) with three color classes: red, white, and black. Specular highlights (shine) and scale texture result in shiny areas of the snake being assigned to the white color center. C: The same beetle specimen (*Chrysochroa mniszechii*) photographed using diffuse (upper row) and direct (lower row) light. Fitting $n = 2$ color centers using k-means clustering produces different color centers and different color patch geometries. D: Batch processing with the same set of color classes. All of these *Polistes fuscatus* wasp faces share a palette of three colors (yellow, reddish brown, and dark brown), but fitting $n=3$ color centers for each image using k-means clustering results in subtly different colors for each image, and they are returned in an arbitrary order. E: Batch processing for image sets with different types and numbers of colors. We chose to fit $n = 4$ colors for each beetle (*Chrysochroa* spp.) in this 5-species dataset, resulting in some images being over-clustered and some being under-clustered. Image sources: Jack Randall (A), Alison Davis-Rabosky (B), Nathan P. Lord (C & E), James Tumulty (D).

103 only a subset of biological questions about color pattern variation, and as a result has
104 more stringent requirements for data and equipment (and thus a higher barrier to entry).
105 We could also find no dedicated tools specifically for making color maps: most methods
106 provide a function or functions for performing color segmentation before running the rest
107 of the analysis, so users who need color maps for any other purpose not yet implemented
108 in these tools need sufficient coding expertise to extract them.

109 The color segmentation problem has proven to be so intractable that quantitative
110 color pattern analysis has mostly been limited to organisms with brightly colored, highly
111 contrasting color patterns on relatively flat and untextured surfaces. This largely limits
112 us to some species of butterflies and poison frogs. As a result, our ability to generate
113 questions and hypotheses about color pattern evolution have far outpaced our ability to
114 quantitatively analyze them.

115 The `recolorize` package is designed to address this problem so that downstream color
116 pattern analysis tools can be used for a wider variety of contexts. We aim to make the
117 package easy to use, easy to modify, and easy to export to other packages and pipelines.
118 The color segmentation options are fast and deterministic, have been tested across a
119 wide variety of images, organisms, and use cases, and are reasonably straightforward in
120 their structure. The general process is: 1. initial clustering step; 2. refinement step; 3.
121 optional semi-manual edits; 4. export to desired format. The resulting toolbox is capable
122 of handling a wide range of images, and has been used successfully in several contexts
123 where k-means clustering has not worked. In order to illustrate that functionality, this
124 paper will go over how to use `recolorize` to generate usable color maps for all of the
125 examples which fail with k-means clustering in Fig. 2.

¹²⁶ **Glossary**

¹²⁷ Terms used for each of the components of this process vary somewhat in the literature;
¹²⁸ here we define what we mean in this paper (and in the package) for reference.

¹²⁹ 1. **Color pattern:** Static visual appearance of the sender, e.g. how colors are arranged
¹³⁰ on the organism, as captured by a single image (or 3D surface).

¹³¹ 2. **Color class:** A specific ID (usually numeric) to which portions of the color pattern
¹³² are assigned.

¹³³ 3. **Color center:** The computer-readable color of the color class, typically expressed
¹³⁴ as an RGB triplet.

¹³⁵ 4. **Color patch:** All the portions of a color pattern which are assigned to the same
¹³⁶ color class.

¹³⁷ 5. **Color space:** The coordinate system (typically three-dimensional) used to repre-
¹³⁸ sent the color of each pixel, and within which color distances are calculated.

¹³⁹ 6. **Color segmentation:** The process of segmenting an image into discrete color
¹⁴⁰ patches.

¹⁴¹ **Results**

¹⁴² Code and images for running each of these examples is provided at https://github.com/hiweller/recolorize_examples. All examples are deterministic, meaning that the code
¹⁴³ as written will produce the same results every time it is run, regardless of the R seed or
¹⁴⁴ computer.

¹⁴⁶ Preparing images for recolorize

¹⁴⁷ Many users of `recolorize` will already have images, and the package is fairly forgiving
¹⁴⁸ of variation due to lighting, texture, or arrangement (e.g., of feathers on a bird) since
¹⁴⁹ we include tools for making post-hoc adjustments. In brief, users should try to control
¹⁵⁰ for as many sources of variation as possible: use the same camera, lighting, background,
¹⁵¹ resolution, positioning, and color standard for the entire dataset.

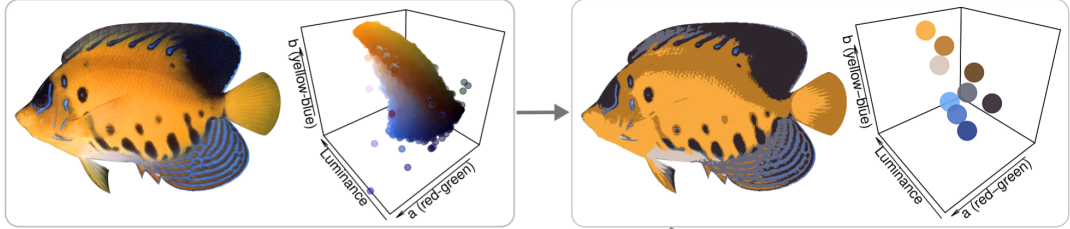
¹⁵² The most important pre-processing step for using `recolorize` is background masking,
¹⁵³ for which there are many existing tools available. The package does not perform back-
¹⁵⁴ ground masking or image segmentation: instead, users should mask out the background
¹⁵⁵ of the image using transparencies (e.g. using GIMP or Photoshop). `Recolorize` can
¹⁵⁶ also ignore a background of uniform color by specifying a range of RGB colors. There
¹⁵⁷ are several tools available for automatic background masking, such as Sashimi ([Schwartz](#)
¹⁵⁸ and [Alfaro, 2021](#)) or Batch-Mask ([Curlis et al., 2021](#)), which could be used for large
¹⁵⁹ image sets. The exception is for the `patternize` workflows we show in examples E and
¹⁶⁰ F below, where the landmark alignment performs automatic background masking on
¹⁶¹ unmasked images.

¹⁶² Examples

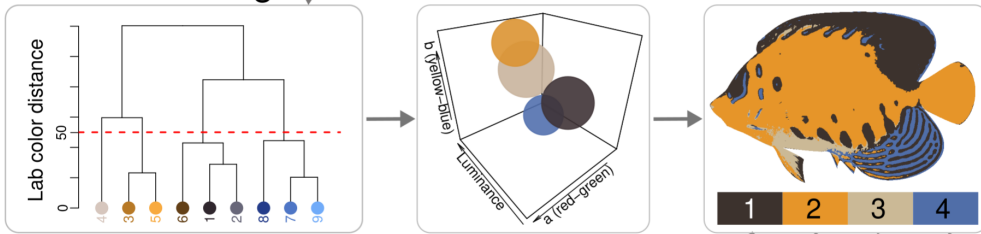
¹⁶³ Example A: Main `recolorize` workflow

¹⁶⁴ The major problem in Fig. 2A is that by fitting $n = 4$ color centers for the angelfish
¹⁶⁵ image, k-means clustering achieves lower within-cluster variances by assigning separate
¹⁶⁶ light and dark yellow color centers (since these take up a greater proportion of the image)
¹⁶⁷ and grouping the white pixels into the light yellow color class, despite the fact that these

A. Initial clustering



B. Reclustering



C. Export



Figure 3: Successful segmentation of the angelfish (*Pygoplites diacanthus*) image from Fig. 2A, illustrating the core steps of the package. A: First, the pixels of the original image are binned by their coordinates in each color channel using a user-selected number of bins per channel using the `recolorize` function. In this case, only 9 of 27 bins had pixels assigned to them. B: These initial bins are combined based on perceived similarity using `recluster` by combining either bins that have a Euclidean distance less than the user-selected cutoff (here, cutoff = 50), or by specifying a final number of colors. The original image is then re-fit using the resulting set of color centers. C: The resulting color map is exported to any of a number of formats. Here, individual color patches are exported as binary masks using the `splitByColor` function.

168 colors are less similar than the dark and light yellow (as indicated by their proximity in
169 3D color space). This is a common issue with k-means clustering that is easily resolved
170 by the basic `recolorize` workflow, so we will use this image to illustrate these steps in
171 detail.

172 The core of the `recolorize` package is a two-step process for color segmentation:
173 first, each pixel in the image is assigned to a region based on ranges defined for each
174 color channel, resulting in what is essentially a 3D histogram of color distribution for
175 the image (Fig. 3A). This is accomplished with the `recolorize` function, using a user-
176 specified number of bins per channel, where the total number of resulting color centers
177 will be n^3 for n bins per channel (here, we used 3 bins per channel resulting $3^3 = 27$
178 possible color regions, only 9 of which contained pixels from the fish image). The color
179 center of each region is then calculated as the average value of all of the pixels assigned
180 to that region (or the geometric center if no pixels were assigned to it). This step requires
181 no distance calculations or color center estimations because pixels are binned into pre-
182 existing regions. As a result, this step is relatively fast and deterministic, and serves to
183 reduce potentially millions of colors in the original image to typically only a few dozen,
184 depending on the user's specification of how finely to bin them.

185 Second, these initial color centers are reduced according to some rule, such as com-
186 bining similar color centers or dropping the smallest color patches. The most generally
187 effective function for this step is the `recluster` function, which calculates the Euclidean
188 distance between all pairs of color centers to which any pixels were assigned. Color cen-
189 ters are then clustered by similarity using hierarchical clustering (R Core Team, 2022),
190 and users provide either a similarity cutoff which determines which colors to combine or

191 a final number of expected colors. In Fig. 3B, we used a cutoff of 50 (Euclidean distance
192 in CIE Lab color space) to combine the 9 initial color centers into 4 consensus color
193 centers. New color centers are calculated as the weighted average of the original color
194 centers being combined, with color patch size as the weights. The `recluster` function
195 then refits the original image with these new color centers.

196 In short, the first step reduces the image to a manageable number of colors, after which
197 more computationally intensive steps (such as calculating a pairwise distance matrix) can
198 be performed deterministically. Because they are also not density dependent, this two-
199 step method also better preserves small but distinct color patches, such as the white patch
200 on the ventrum of the fish image. Finally, the color map can be exported to a variety of
201 formats and packages. In Fig. 3C, we export the color map as a stack of binary masks (0
202 = color absence, 1 = color presence), but the later examples will illustrate functions for
203 exporting to specific packages.

204 **Example B: More complex segmentation**

205 The coral snake from Fig. 2B represents a more complex example, because the specular
206 highlights created by the shiny scales of the snake appear white regardless of their loca-
207 tion on the snake (so they cannot be combined with appropriate color centers based on
208 similarity). Instead, we first blur the image to reduce minor color variation due to the
209 scale texture using `blurImage`, then produce an initial color map using `recolorize` and
210 `recluster` as in the prior example, resulting in four color centers (Fig. 4). Note that color
211 center 1 (a medium gray) contains most of the specular highlights; remaining portions
212 of the highlight have been assigned to color center 4. This is a fairly common problem

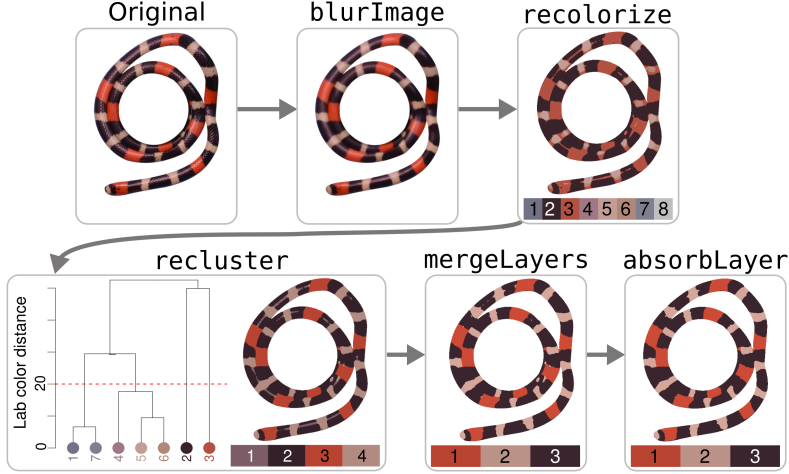


Figure 4: Successful segmentation of the coral snake (*Micrurus* sp.) image from Fig. 2B. This image requires more steps to deal with color variation due to scales and specular highlights: first we blur the image using `blurImage` to mitigate the scale texture, then call `recolorize` (2 bins per channel = $2^3 = 8$ color centers) and `recluster` (cutoff = 20) to perform segmentation. The `mergeLayers` function allows us to specifically combine color centers 1 and 2 (becoming the new color class 3), which eliminates much but not all of the specular highlights. Finally, the `absorbLayer` function eliminates the remaining specular highlights by absorbing isolated speckles from patch 2 into the surrounding color patches.

213 in color segmentation output: the method mostly works, but has small problems that
 214 render the color map ineffective, with no easy way for users to modify it. For this rea-
 215 son, the `recolorize` package also includes tools for modifying color maps in specific,
 216 reproducible ways. First, we can combine color centers 1 and 2 using the `mergeLayers`
 217 function. Second, to clean up the small areas of highlight which were assigned to color
 218 center 4, we use the `absorbLayer` function: this targets areas of a color patch within a
 219 user-specified area and/or location boundary, and changes the color of each separate area
 220 to that of the color patch with which it shares the longest border, effectively “absorbing”
 221 stray speckles.

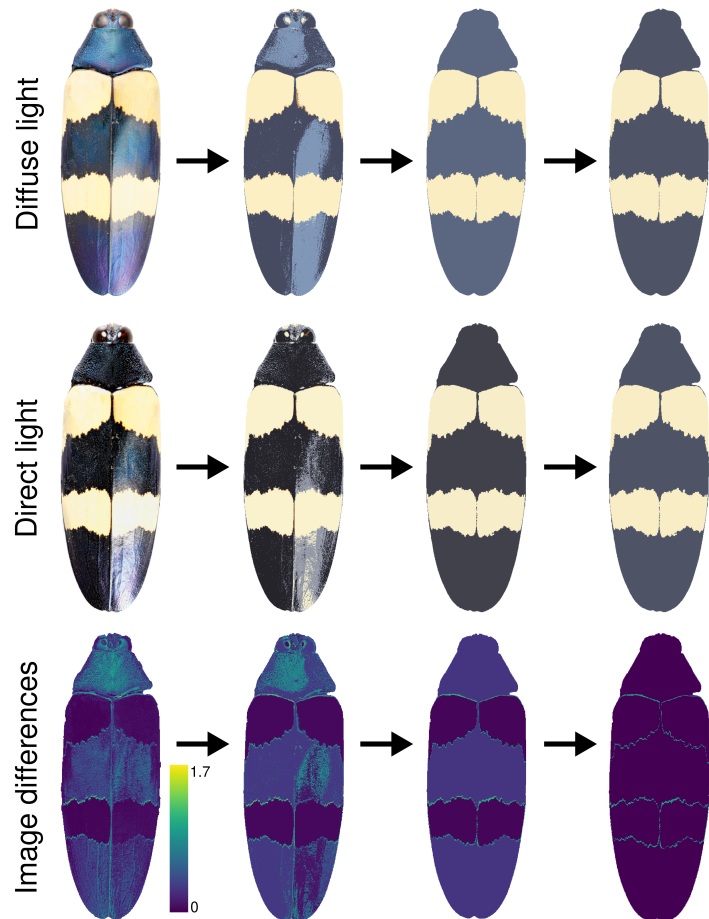


Figure 5: Using `recolorize` to recover the same color pattern information from photos with different lighting conditions. Top row: steps for producing a color map for the diffuse light image. Middle row: steps for the direct light image. Bottom row: differences between the images (calculated using the `imDist` function).

222 Example C: Lighting variation

223 Although the ideal image set is acquired using the same camera, lighting conditions, and
224 color standards, users will often have images accumulated from a range of sources where
225 these variables cannot be controlled, e.g. images taken from the iNaturalist database
226 (Nugent, 2018) or by different lab members over several years of a field season. Although
227 the actual color of the image cannot be used for analysis, these images still contain
228 information: we can measure the spatial distribution of colors to quantify color pattern
229 variation, e.g. with `patternize` (Van Belleghem et al., 2018).

230 Fig. 2C provides a good example of this problem: we know that these images contain
231 identical color pattern information (since this is the same specimen), but the colors
232 themselves vary from a purplish-blue under diffuse light to black with intense specular
233 highlights under direct light. Although k-means clustering produces a dark and a light
234 cluster for each image, the color centers themselves are not only quite different, but
235 the color patches are very different in shape due to the highlights. In this case, we
236 can use `recolorize` (following a similar procedure to that in Fig. 4) to correct for that
237 difference and produce two near-identical color maps from the two images, recovering the
238 same spatial information for the distribution of the light and the dark colors (Fig. 5).
239 Although even in this case the two final maps are not perfectly identical—the borders
240 between the light and dark patches differ slightly (Fig. 5, bottom right)—only 3,270 of
241 219,107, about 1.5%, of the pixels are assigned differently in each image.

²⁴² **Example D: Pattern analysis with patternize**

²⁴³ Users will often need to map each image in a dataset to the same color palette in order
²⁴⁴ to compare differences in color pattern distribution. The `patternize` package (Van Bel-
²⁴⁵ leghem et al., 2018) implements this approach: images are aligned to a common sampling
²⁴⁶ grid (a `RasterStack`) using image registration or landmarks, mapped to a common color
²⁴⁷ palette, and then analyzed with principal components analysis (PCA). This method is
²⁴⁸ probably the closest available equivalent to geometric morphometrics with color pattern
²⁴⁹ analysis, because the alignment step allows us to control for variation in shape, orienta-
²⁵⁰ tion, and size before analyzing variation in color pattern.

²⁵¹ In practice, the most difficult step of using `patternize` is often the color segmenta-
²⁵² tion. Like several other color analysis packages and tools, `patternize` mostly relies on
²⁵³ k-means clustering to extract color patches from images (especially for batch process-
²⁵⁴ ing), which can fail for any of the reasons outlined above. Instead, we can combine the
²⁵⁵ strengths of `patternize` and `recolorize` by using `patternize` to perform the image
²⁵⁶ alignment step and `recolorize` to do the color segmentation. Here we show a working
²⁵⁷ example using *Polistes fuscatus* wasp face images, a subset used with permission from
²⁵⁸ Tumulty et al. (2021). We landmarked the original images (Fig. 6A) in ImageJ, using a
²⁵⁹ simple scheme of only 8 landmarks, along with masking polygons to restrict our analyses
²⁶⁰ to the frons and clypeus of the head (Fig. 6B). These were passed through the `alignLan`
²⁶¹ function in `patternize` to produce a list of aligned `RasterBrick` objects. We converted
²⁶² these to image arrays using the `brick_to_array` function in `recolorize`, determined a
²⁶³ universal color palette using an initial color segmentation of all images (Fig. 5C), then
²⁶⁴ used the `imposeColors` function to map all aligned images to the same set of colors

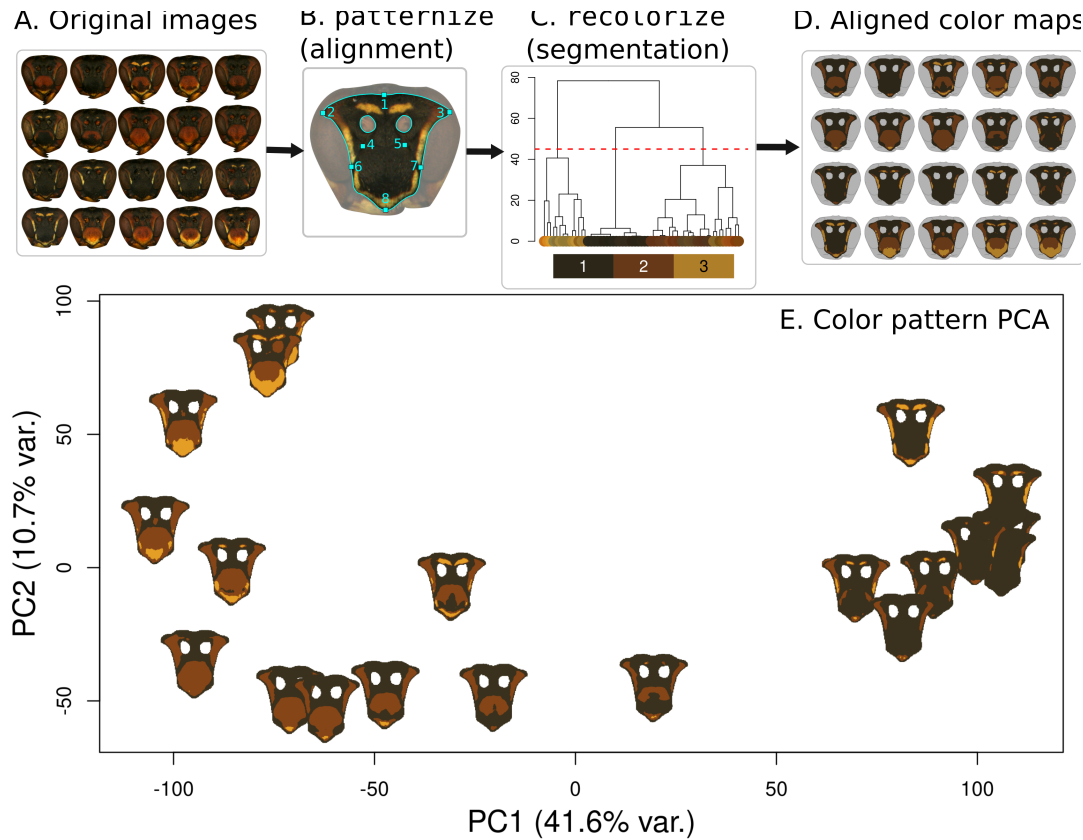


Figure 6: Process for combining `recolorize` and `patternize` to run a whole-color-pattern principal components analysis (PCA). A: Original images of *Polistes fuscatus* wasp faces, taken with the same lighting and camera conditions. B: Landmarking scheme for alignment. C: Generating a universal color palette from color segmentation on individual images. D: Applying the universal color palette using the `imposeColors` function to generate color maps. E: Color pattern PCA as generated by aligned, segmented images, characterizing color pattern diversity among the wasp face images.

265 (Fig. 5D). Finally, we converted these color maps back to `patternize` rasters using the
 266 `recolorize_to_patternize` function and used the `patPCA` function in `patternize` to per-
 267 form a whole color pattern PCA (Fig. 5E). A complete version of this example—including
 268 step-by-step code to reproduce it and more detailed explanations—is available here:
 269 <https://hiweller.rbind.io/post/recolorize-patternize-workflow/>.

270 **Example E: Spectral analysis with pavo**

271 Even under ideal circumstances (identical lighting and camera setups, color correction,
272 camera calibration, etc), color images do not provide full-spectrum color information.
273 Instead, they are limited to the visible spectrum and biased toward human visual sensi-
274 tivities—any user interested in non-human visual perception cannot rely on traditional
275 RGB image data alone to test their questions. One relatively cheap and accessible solu-
276 tion to this problem is to combine color maps, which provide spatial information, with
277 reflectance measurements taken with a point spectrometer.

278 Reflectance spectra provide a more objective measurement of color and capture wave-
279 lengths outside the range of human perception (ultraviolet, 300-400 nanometers) without
280 the expense of obtaining a UV photography set-up. If users have reflectance spectra,
281 the color standardization in their images is less important (so long as spectra can still
282 be accurately assigned to the corresponding color patch). For example, if photos and
283 reflectance spectra were obtained from the same individuals but under variable light-
284 ing conditions or camera setups, reflectance spectra could be used to retroactively apply
285 color-standardized data to the images. But because they are point measurements, spec-
286 tral data cannot provide spatial information. This is part of the workflow of the pavo
287 package ([Maia et al., 2019](#)), which enables users to combine spatial and spectral informa-
288 tion by providing visual models (based on reflectance spectra) in combination with color
289 maps. As with `patternize`, the pavo package relies primarily on k-means clustering to
290 do the color segmentation, meaning users encounter many of the pitfalls illustrated in
291 earlier examples.

292 Here, we illustrate the combination of reflectance spectra with `recolorize` using an

example dataset of birds, flowerpiercers in the genus *Diglossa* (Fig. 7A), which have striking examples of color pattern repetition within and between species (Remsen Jr, 1984; Vuilleumier, 1969) and colors outside of the human visual spectrum. Birds exhibit nearly all of the features which we have shown tend to foil k-mean clustering (Mason et al., 2021). The most common type of bird specimen preparation (aptly termed a ‘round skin’) is convex, with contours that photograph as color variation similar to Fig. 2A; different arrangements of feathers create textures and irregular shadows and shine as in Fig. 2B; and many bird species have finescale color pattern elements like speckles, wingbars, or facial markings which will usually be absorbed by larger color patches. These features make it difficult to combine reflectance spectra with useful color maps.

We followed the same procedure as in example D to generate the color maps for the birds. To identify a universal color palette to which bird images should be mapped, we measured reflectance spectra in five locations on the breast of each bird and grouped spectra with similar shapes as calculated using the `peakshape` function in `pavo` (Fig. 7B). In this case, because the reflectance spectra indicated that the navy blue color (color center 5) had higher UV reflectance than the black (color center 1), we kept these as separate color centers although they were very similar in RGB color—an example of using outside information to inform our choice of color palette. We processed bird images through `patternize` and `recolorize` as in Fig. 5 to control for shape variation, then converted the color maps to classify objects using `recolorize_classify` (Fig. 7C).

To combine these color maps with spectral data, we first calculated aggregate reflectance spectra using `procspec` and `aggspcpec` in `pavo`, resulting in 5 reflectance curves corresponding to the 5 color centers in the color maps. We used this reflectance data to

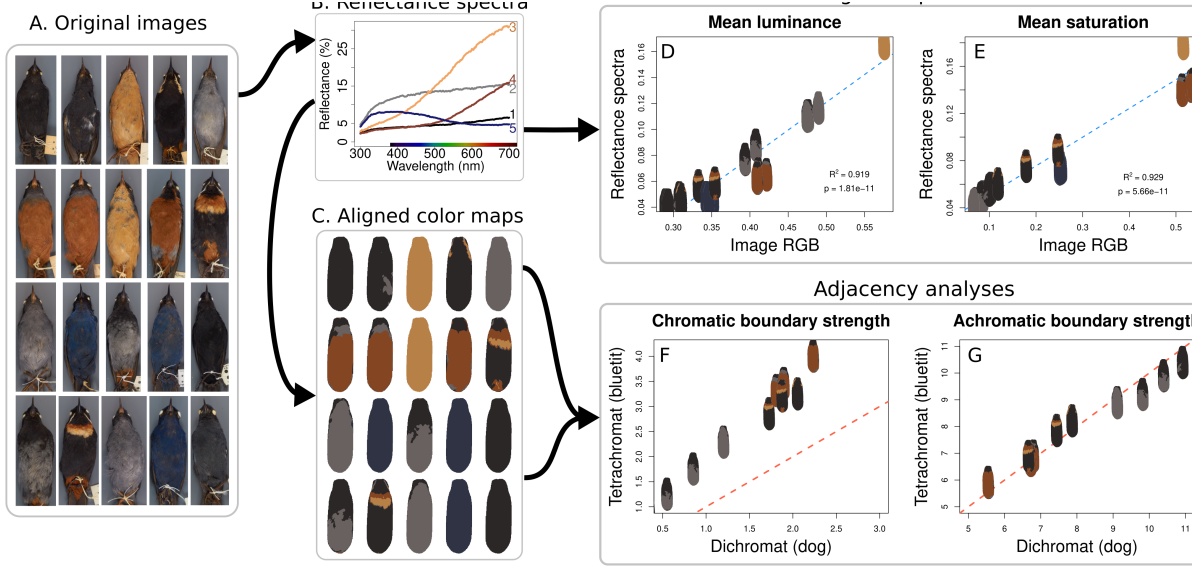


Figure 7: Combining color maps with spectral data in *pavo*. A: Original images of *Diglossa* spp. birds. B: Reflectance spectra used to determine the five color classes for color segmentation (black, gray, yellow, brown, and blue). C: Color maps (generated in a similar manner to Fig. 6) mapping each bird breast to one of the five color classes. D-E: Comparison of mean luminance and saturation results using image data and spectral data. Blue lines are linear regression fits. F-G: Comparisons of Endler's adjacency analysis as performed in *pavo* for a dichromat and a tetrachromat (Maia et al., 2019; Endler, 2012). The red dashed line represents a slope of 1 and intercept of 0; points on this line would indicate identical values for the two visual systems. Chromatic boundary strength = color contrast, achromatic boundary strength = luminance (brightness) contrast. Specimens from left to right: row 1 LSUMZ 85389, LSUMZ 90468, LSUMZ 91068, LSUMZ 98863, LSUMZ 98873; row 2 LSUMZ 33373, LSUMZ 33374, LSUMZ 38886, LSUMZ 79148, LSUMZ 80877; row 3 LSUMZ 189657, LSUMZ 196409, LSUMZ 228146, LSUMZ 229100, LSUMZ 229115; row 4 LSUMZ 125407, LSUMZ 129286, LSUMZ 163814, LSUMZ 174295, LSUMZ 179214.

316 generate visual models and color distance objects using the `vismodel` and `coldist` func-
 317 tions from the *pavo* package (Maia et al., 2019), here focusing on visual models for a
 318 UV-sensitive tetrachromat (bluetit, as provided by *pavo*) and a dichromat (dog).

319 We then combined spectral and spatial data by running the `adjacent` function in
 320 *pavo*, which performs Endler's adjacency analyses, using these visual models and our
 321 `recolorize`-generated color maps. For comparison, we also ran adjacency analysis using
 322 the intrinsic RGB colors of the actual color maps, rather than spectral data, which is a

323 simplifying assumption made by the `recolorize_adjacency` function in the absence of
324 spectral data.

325 We found that the mean luminance and saturation calculated using the intrinsic RGB
326 colors were tightly correlated with these values as calculated using reflectance spectra (R^2
327 = 0.919 and 0.929, respectively), although the scales of these values were quite different for
328 the two methods (Fig. 7D-E). When comparing between dichromatic and tetrachromatic
329 visual systems, we found that the chromatic (color contrast) boundary strength scores
330 differed substantially, with the tetrachromatic visual system having universally higher
331 chromatic boundary strength scores. Interestingly, the achromatic (brightness contrast)
332 boundary strength scores were nearly identical for the two visual systems (Fig. 7F-G).

333 This example is undoubtedly the most complex of those we present here. We used
334 `patternize`, `recolorize`, and `pavo` to combine spatial and spectral data, analyzing
335 images which pose many of the problems that traditional segmentation methods can-
336 not resolve, and calculating biologically relevant metrics for two different visual models.
337 `Recolorize` worked well for classifying and grouping color patches both within and be-
338 tween species, without the loss of the fine scale pattern information (e.g., the chest bands
339 and mustaches), thus addressing many of the ‘signal-to-noise’ problems that have been a
340 bottleneck for color pattern analysis in birds. Additionally, by integrating `recolorize`
341 with `pavo` we were able to successfully combine spectral data with visual photographs to
342 get a more accurate representation of colors with reflectance in the UV range, a critical
343 component to quantifying color data for taxa like birds which detect colors outside of the
344 human visual range.

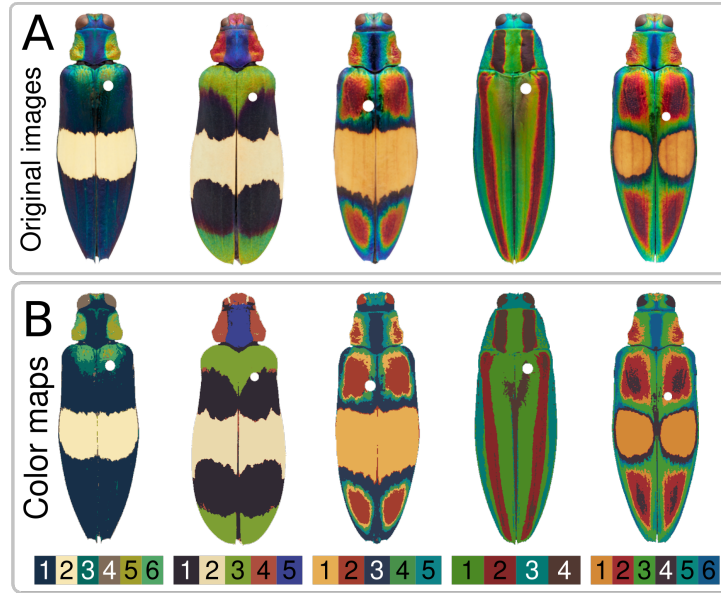


Figure 8: Color maps for *Chrysochroa* spp. beetles, generated by the same series of `recolorize` calls for different images. A: Original images. The white spot on each beetle is where the insect pin was masked with transparency before loading the images into the package. B: Resulting color maps, which range from 4 to 6 colors for each image in this case. Image sources: Nathan P. Lord.

345 **Example F: Batch processing with different colors**

346 Our final example illustrates an aspect of the `recolorize` workflow which works well for
347 batch processing an image set that does not have a shared color palette. When dealing
348 with a set of images where not each image can be mapped to the same set of colors—for
349 example, a comparative dataset consisting of images of different species—researchers must
350 either fit the same number of color centers to each image, resulting in over- and under-
351 clustered images (see Fig. 2D) or choose a different number of colors for each individual
352 image, meaning they have to invent some criterion for determining how many colors
353 to assign each image. In practice, these criteria tend to be fairly subjective. Because
354 the automatic `recolorize` functions operate by grouping colors together by similarity,
355 applying the same series of `recolorize` calls to each image produces a different number
356 of color centers depending on the image (Fig. 8).

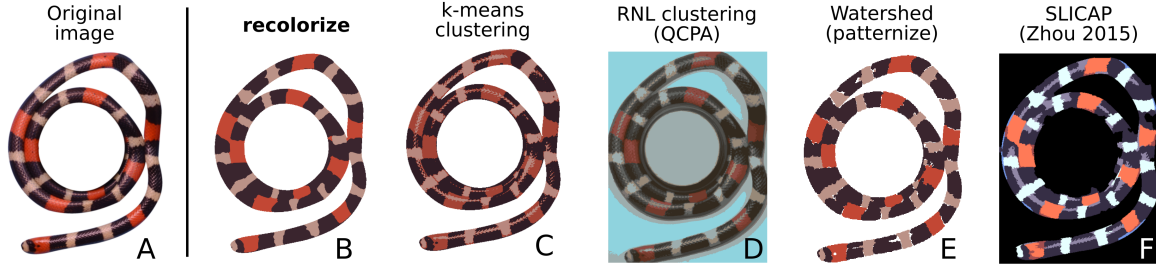


Figure 9: Comparison of recolorize with three other methods for organismal color segmentation. A: Original image. B: Recolorize output as achieved in Fig. 4. C: One run of k-means clustering output. D: Output from receptor noise-limited (RNL) clustering as implemented by the QCPA framework in micaToolbox (van den Berg et al., 2020; Troscianko and Stevens, 2015). E: Watershed segmentation of three colors in patternize (separate layers are superimposed). F: Simple linear iterative clustering with affinity propagation (SLICAP) segmentation as described by Zhou (2015) and implemented by Lampros (2021)

357 These color maps are imperfect: each beetle in the dataset has a different relationship
358 between texture, shine, and color, which cannot easily be automated in the same call.
359 The initial `recolorize` call could be used to determine the color classes for each image,
360 but users should still go through color maps and make individual modifications as-needed.

361 Comparison with existing methods

362 Although k-means clustering is the most widely used method for color clustering in im-
363 ages, here we compare recolorize to a number of other methods that researchers might
364 encounter when searching for color segmentation solutions (Fig. 9). We summarize the
365 major differences in color clustering methods discussed in this paper in Table 1. In com-
366 parison to the other methods, because recolorize includes tools for modifying output that
367 is close to satisfactory, users do not need to find a single solution that will perfectly seg-
368 ment all of their images; they can modify output on a per-image basis, the steps of which
369 are all recorded in the recolorize object for repeatability (see below section on object

370 structure).

371 **Receptor noise-limited clustering**

372 The ImageJ plugin micaToolbox ([Troscianko and Stevens, 2015](#)) and accompanying
373 Quantitative Color Pattern Analysis toolkit ([van den Berg et al., 2020](#)) are among the
374 most comprehensive tools widely available to biologists for modeling non-human visual
375 systems. One option in the toolkit is receptor noise-limited (RNL) color clustering,
376 which uses perceptual thresholds of a specified visual system to cluster an image based
377 on whether a given viewer could distinguish colors at a specified viewing distance. To
378 run RNL clustering, we used a camera RAW image of the snake that included a 40%
379 reflectance standard, as well as calibrating the camera using a separate image of an Xrite
380 Colorchecker. We then generated a multispectral image, used region-of-interest (ROI)
381 masking to analyze only the snake, performed acuity correction for a viewing distance
382 of one meter, converted to a cone-catch image (we chose a human model for comparison
383 with other methods), ran the RNL ranked filter, and finally RNL clustering ([van den Berg](#)
384 [et al., 2020](#); [Caves and Johnsen, 2018](#)). The resulting image includes some background
385 (despite the ROI implementation) and segments the snake itself into 19 color clusters.
386 With ROI masking, processing this image took three minutes on a personal laptop with
387 16Gb RAM (not accounting for user error); without ROI masking, the image took over
388 20 minutes to process.

389 **Watershedding in patternize**

390 The watershedding algorithm as implemented in patternize is intended to solve prob-
391 lems of shine and texture on an image. Although the watershed output (as implemented
392 by the patLanW function in patternize) is usable, it requires repeated user input (clicking

393 on the original image to set seeds for each discrete color patch, e.g. every black segment
394 of the snake) for each color cluster, and in this case the results still do not completely
395 solve the specular reflectance problem (Fig. 9D), meaning in this case the method is both
396 less effective and more subjective.

397 **General color segmentation algorithm**

398 We also attempted to use an algorithm for general color segmentation of images as
399 described by Zhou (2015), termed simple linear iterative clustering with affinity propa-
400 gation (SLICAP). Given that this method also does not require any a priori specification
401 of the expected number of colors, it performs remarkably well (producing 6 color clusters
402 not counting the background), but still results in many color clusters with no easy way
403 for users to modify the output.

404 **Package installation, structure, and input**

405 **Installation**

406 The most recent stable release version of the package can be installed from the Compre-
407 hensive R Archive Network (CRAN) from R using the `install.packages()` function:

```
408 1 install.packages("recolorize")
```

409 The development version of the package can be installed from GitHub (<https://github.com/hiweller/recolorize>) using the `devtools` package (Wickham et al., 2021):

```
411 1 devtools::install_github("hiweller/recolorize")
```

412 The recolorize class

413 The `recolorize` package mostly works with R objects of S3 class `recolorize`, which are

414 output by the base functions and which most functions in later steps of the workflow will

415 take in as an argument. Objects of this class are lists with the following elements:

416 1. `original_img`: The original image, stored as a raster array (essentially a matrix of

417 hexadecimal codes).

418 2. `centers`: A matrix of color centers, listed as one RGB triplet per row in a 0-1

419 range. These are usually the average color of all pixels assigned to that color class

420 unless otherwise specified by the user.

421 3. `sizes`: The number of pixels assigned to each color class.

422 4. `pixel_assignments`: A matrix of color class assignments for each pixel. For exam-

423 ple, all pixels coded as 1 in the `pixel_assignments` matrix are assigned to color

424 class 1 (which will be row 1 of `centers`).

425 5. `call`: The set of commands that were called to generate the `recolorize` object.

426 The call is especially helpful for reproducibility, because it stores every step used to

427 generate the current segmentation (any function that returns a `recolorize` class object

428 will modify the call element accordingly).

429 Discussion

430 Fully automated methods rarely work all of the time, and are difficult to modify, while

431 fully manual methods are subjective and time-consuming. `Recolorize` strikes a balance

	recolorize	k-means clustering	RNL clustering	Watershed	SLICAP
Images from multiple sources	Y	Y		Y	Y
No calibration required	Y			Y	Y
Automated clustering options	Y		Y		Y
Tools for modifying output	Y				
Deterministic	Y		Y		Y
Batch processing (diff. colors)	Y	Y	Y		Y
Batch processing (same colors)	Y	+		Y	
Export directly to other methods	Y				
Supports transparencies	Y				+
Multispectral images			Y		
Non-human visual systems			Y		
Graphical user interface			Y	Y	

432 between these two extremes by providing an effective color segmentation algorithm along
433 with tools for modifying and exporting the resulting color maps. In the simplest case,
434 users only have to tinker with the number of initial color centers in the first step and the
435 similarity cutoff in the second step. Even in more complicated cases, where color maps are
436 modified individually, these steps are recorded in the call element of the `recolorize` ob-
437 jects. This design allows `recolorize` to handle a much wider range of color segmentation
438 problems than it could otherwise.

439 Comparison and complementarity with existing methods

440 Most of the methods to which we compared `recolorize` are implemented in existing
441 pipelines, and are therefore not the sole focus of the software or method in question. For
442 example, the RNL clustering output in Fig. 9C requires specific calibration equipment,
443 knowledge of visual system parameters, and ten processing steps to achieve a 19-cluster
444 color map. The results are accurate to human perception: portions of the snake are dif-
445 ferent colors due to shine and 3D contour, which would be detectable to a human viewer.
446 However, the extra equipment and number of steps required for processing are prohibitive

447 given the research context. This would restrict the analysis to images taken using the
448 same camera and which include a relatively expensive calibration standard, and while the
449 results are highly informative for visual perception, users would have to do substantial
450 modification to measure, for example, the proportion of black on the snake's body, or
451 the length of the border shared between the red and white patches, since each of these
452 is broken up into multiple clusters which sometimes span more than one color. This is
453 because the QCPA workflow in general is concerned with simulating non-human visual
454 systems, which requires a higher standard of calibration and more carefully controlled
455 data collection.

456 Because `recolorize` is a dedicated toolbox for organismal color segmentation, it is
457 designed not as a replacement for existing pipelines but as a complement to them. By
458 making color segmentation more feasible and providing export options to a variety of
459 formats for multiple user cases, `recolorize` makes other color analysis tools easier to use
460 for a wider variety of projects and images.

461 Current and potential applications for `recolorize`

462 Currently, `recolorize` works with PNG and JPEG images, and does not support less
463 common (but more information-rich) formats, such as the multispectral images gener-
464 ated with micaToolbox ([van den Berg et al., 2020](#)) or Image Calibration Analysis Tool-
465 box ([Troscianko and Stevens, 2015](#)). However, the underlying package structure can be
466 extended to other formats as the central algorithms of the package can be modified to
467 images with more than 3 channels, and intermediate steps are exported as their own
468 functions (in addition to being called on by `recolorize()`). For example, we recently

469 used `recolorize` functions for color segmentation of 3D objects (STL files output from
470 photogrammetry; Christopher Taylor, pers. comm.). Such future developments, often
471 driven by specific user cases, will be made available on GitHub.

472 The `recolorize` toolbox can be used to process a high number of images more con-
473 sistently than existing manual or simple automated methods, but its output is imperfect.
474 Users are invariably going to have to tweak problem images or do some things manually
475 if they want 100% efficacy, and will otherwise have to accept some amount of error. In
476 some ways this is about choosing your source of error: computer or user?

477 The relative ease with which we can combine color maps with spectral data (per ex-
478 ample E) also suggests interesting possibilities. Even in this reduced example, when we
479 compare chromatic and achromatic boundary strength for the tetrachromat and dichro-
480 mat, we see that chromatic boundary strength (color contrast) is measurably different
481 between the two visual systems (generally higher for the tetrachromat than the dichro-
482 mat), which we would expect. However, we also see that the two visual systems are very
483 closely matched in achromatic boundary strength (brightness contrast), which suggests
484 that achromatic boundary strength depends less on particular properties of a given visual
485 system than chromatic boundary strength. When we measured mean luminance and sat-
486 uration from reflectance spectra versus intrinsic RGB colors, we found tight correlations
487 (but different scales) for the two sets of measurements. In this case, because the Diglossa
488 dataset contains high-quality images acquired under consistent settings, it would not be
489 wildly unreasonable to use the intrinsic RGB colors if spectral data were unavailable.
490 This approach must be used with caution, especially if researchers know of (or are un-
491 certain about) a substantial UV-reflective component of the color patterns in question,

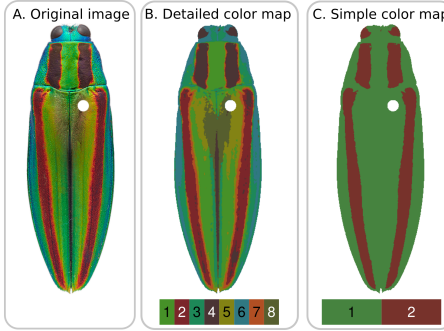


Figure 10: Different color maps generated for the same image. Solution depends on the use case. Image: Nathan P. Lord.

492 or if the images are from different sources.

493 A last possibility would be to use `recolorize` to generate a training set for a machine
494 learning approach. These generally have the problem, especially in fields like organismal
495 biology, that the amount of training data and expertise required to get a sufficiently
496 trained algorithm is actually more effort than just doing everything manually (given that
497 it usually has limited applicability). Performing the segmentation in `recolorize` might
498 make it easier to generate that training data so this solution could be used for more
499 specific problems.

500 The 'correct' color map depends on the question

501 Image segmentation is a classically difficult problem in computer vision, especially be-
502 cause there is no single 'correct' answer for appropriate color pattern segmentation. A
503 color map is by definition a simplified representation of an actual color pattern, so the
504 correct solution is not intrinsic to the image, but depends on the user's question. For
505 example, in Fig. 10, we illustrate two possible color segmentations for our original image
506 of an iridescent jewel beetle (*Chrysochroa fulgidissima*). In Fig. 10B, we show a more

507 complex, 8-color segmentation, which retains the brighter orange on the borders of the
508 red stripes, and fits different shades of red and blue to reflect differences in viewing angle
509 of the iridescent elytra. This color map would be appropriate for answering questions of
510 visual contrast and perception, since it retains more properties relevant for visual stimuli.
511 In Fig. 10C, we show a much simpler 2-color segmentation, consisting only of red and
512 green. This is not a very visually faithful representation of the original image, but if
513 we wanted to measure the location and distribution of green iridescence across beetle
514 taxa, this map would be much more helpful to us than that in Fig. 10B. We end on this
515 example to emphasize that there is no universal solution for the problem of biological
516 color segmentation: there is no method so comprehensive that it absolves researchers of
517 posing specific questions.

518 Acknowledgements

519 We are grateful to James Tumulty, Alison Davis-Rabosky, and Able Chow for providing
520 images used as examples. Christopher Taylor, Ghislaine Cardenas-Posada, Matthew
521 Fuxjager, John Capano, and Nicole Moody provided helpful feedback on the first draft
522 of the paper. Thank you to the Louisiana State University (LSU) color seminar group
523 and Brant Faircloth for sparking the discussions that led to this paper. Thanks to Robb
524 Brumfield, Nick Mason, and the LSU Museum of Natural Science for access to and
525 resources for photographing bird specimens. Lastly, we would like to thank HIW's PhD
526 advisor, Elizabeth Brainerd, for providing HIW with the academic freedom and gentle
527 but needed encouragement to pursue this project.

528 **Funding**

529 Funding was provided by NSF Graduate Research fellowships to HIW and AEH (DEG
530 2040433), NSF DEB #1841704 to NPL, the Bushnell Fund at Brown University to HIW,
531 and a Doctoral Dissertation Enhancement Grant from Brown University to HIW. Any
532 opinion, findings, and conclusions or recommendations expressed in this material are
533 those of the authors and do not necessarily reflect the views of the National Science
534 Foundation.

535 **Attributions**

536 HIW wrote the package, example code, and manuscript. NPL provided images, feed-
537 back, funding, and helped write MS. AEH provided bird data (images and spectra) and
538 helped write the manuscript. SMVB helped extend the package to be compatible with
539 `patternize` and helped with coding, especially in the wasp example, and edited the
540 manuscript.

541 **Competing Interests**

542 The authors declare no competing interests.

543 **Data availability**

544 The development version of the package is available on GitHub: <https://github.com/>
545 [hiweller/recolorize](https://github.com/hiweller/recolorize). The stable release version is available on the Central R Archive

546 Network: <https://cran.r-project.org/package=recolorize>. All images and code
547 used to generate the examples are available in a separate Github repository: https://github.com/hiweller/recolorize_examples.
548

549 References

550 Dean C. Adams and Erik Otárola-Castillo. geomorph: an r package for the collection and
551 analysis of geometric morphometric shape data. *Methods in Ecology and Evolution*, 4
552 (4):393–399, 2013. doi: <https://doi.org/10.1111/2041-210X.12035>. URL <https://besjournals.onlinelibrary.wiley.com/doi/abs/10.1111/2041-210X.12035>.
553

554 Dean C Adams, F James Rohlf, and Dennis E Slice. Geometric morphometrics: ten years
555 of progress following the ‘revolution’. *Italian Journal of Zoology*, 71(1):5–16, 2004.
556

556 H.W. Bates. *A Naturalist on the River Amazons*. John Murray, 1863.
557

557 I. Bekker, F. Sylburg, and K.F. Neumann. *Historia animalium*. Aristotelis Opera.
558 e Typographeo academico, 1837. URL <https://books.google.com/books?id=2Z8NAAAYAAJ>.
559

560 Fred L Bookstein. Combining the tools of geometric morphometrics. In *Advances in
561 morphometrics*, pages 131–151. Springer, 1996.
562

562 Eleanor M Caves and Sönke Johnsen. Acuityview: An r package for portraying the effects
563 of visual acuity on scenes observed by an animal. *Methods in Ecology and Evolution*, 9
564 (3):793–797, 2018.

565 Ian ZW Chan, Martin Stevens, and Peter A Todd. Pat-geom: a software package for the
566 analysis of animal patterns. *Methods in Ecology and Evolution*, 10(4):591–600, 2019.

567 John David Curlis, Timothy Renney, Alison R Davis Rabosky, and Talia Y Moore. Batch-
568 mask: An automated mask r-cnn workflow to isolate non-standard biological specimens
569 for color pattern analysis. *bioRxiv*, 2021.

570 John A. Endler. A framework for analysing colour pattern geometry: Adjacent colours.
571 *Biological Journal of the Linnean Society*, 107(2):233–253, 2012. ISSN 00244066. doi:
572 10.1111/j.1095-8312.2012.01937.x.

573 John A. Endler, Gemma L. Cole, and Alexandria M. Kranz. Boundary strength analysis:
574 Combining colour pattern geometry and coloured patch visual properties for use in
575 predicting behaviour and fitness. *Methods in Ecology and Evolution*, 9(12):2334–2348,
576 2018. ISSN 2041210X. doi: 10.1111/2041-210X.13073.

577 Briana D Ezray, Drew C Wham, Carrie E Hill, and Heather M Hines. Unsupervised
578 machine learning reveals mimicry complexes in bumblebees occur along a perceptual
579 continuum. *Proceedings of the Royal Society B*, 286(1910):20191501, 2019.

580 Felipe M. Gawryszewski. Color vision models: Some simulations, a general n-dimensional
581 model, and the colourvision r package. *Ecology and Evolution*, 8(16):8159–8170, 2018.
582 doi: <https://doi.org/10.1002/ece3.4288>. URL <https://onlinelibrary.wiley.com/doi/abs/10.1002/ece3.4288>.

584 John A Hartigan and Manchek A Wong. Algorithm as 136: A k-means clustering al-
585 gorithm. *Journal of the royal statistical society. series c (applied statistics)*, 28(1):
586 100–108, 1979.

587 Sarah E Hooper, Hannah Weller, and Sybill K Amelon. Countcolors, an r package for
588 quantification of the fluorescence emitted by pseudogymnoascus destructans lesions on
589 the wing membranes of hibernating bats. *Journal of Wildlife Diseases*, 56(4):759–767,
590 2020.

591 Sönke Johnsen. *The optics of life*. Princeton University Press, 2012.

592 Christian Peter Klingenberg. Morphoj: an integrated software package for geometric
593 morphometrics. *Molecular ecology resources*, 11(2):353–357, 2011.

594 Mouselimis Lampros. *SuperpixelImageSegmentation: Image Segmentation using Su-*
595 *perpixels, Affinity Propagation and Kmeans Clustering*, 2021. URL <https://CRAN.R-project.org/package=SuperpixelImageSegmentation>.

596

597 A Michelle Lawing and P David Polly. Geometric morphometrics: recent applications to
598 the study of evolution and development. *Journal of Zoology*, 280(1):1–7, 2010.

599 Rafael Maia, Hugo Gruson, John A Endler, and Thomas E White. pavo 2: new tools for
600 the spectral and spatial analysis of colour in r. *Methods in Ecology and Evolution*, 10
601 (7):1097–1107, 2019.

602 Nicholas A Mason, Eric A Riddell, Felisha Romero, Carla Cicero, and Rauri CK
603 Bowie. Plumage balances camouflage and thermoregulation in horned larks (eremophila
604 alpestris). *BioRxiv*, 2021.

605 Jill Nugent. inaturalist. *Science Scope*, 41(7):12–13, 2018.

606 Aaron M Olsen and Mark W Westneat. Stereomorph: An r package for the collection

607 of 3d landmarks and curves using a stereo camera set-up. *Methods in Ecology and*
608 *Evolution*, 6(3):351–356, 2015.

609 Anna Orteu and Chris D. Jiggins. The genomics of coloration provides insights into adap-
610 tive evolution. *Nature Reviews Genetics*, 21(8):461–475, 2020. ISSN 14710064. doi: 10.
611 1038/s41576-020-0234-z. URL <http://dx.doi.org/10.1038/s41576-020-0234-z>.

612 P David Polly, A Michelle Lawing, Anne-Claire Fabre, and Anjali Goswami. Phylogenetic
613 principal components analysis and geometric morphometrics. *Hystrix*, 24(1):33, 2013.

614 E.B. Poulton. *The Colours of Animals: Their Meaning and Use, Especially Considered*
615 *in the Case of Insects*. International scientific series. D. Appleton, 1890. URL <https://books.google.com/books?id=Uf4vAAAAYAAJ>.

616

617 R Core Team. *R: A Language and Environment for Statistical Computing*. R Foundation
618 for Statistical Computing, Vienna, Austria, 2022. URL <https://www.R-project.org/>.

619

620 JV Remsen Jr. High incidence of "leapfrog" pattern of geographic variation in andean
621 birds: implications for the speciation process. *Science*, 224(4645):171–173, 1984.

622 Shawn T Schwartz and Michael E Alfaro. Sashimi: A toolkit for facilitating high-
623 throughput organismal image segmentation using deep learning. *Methods in Ecology*
624 *and Evolution*, 12(12):2341–2354, 2021.

625 Jolyon Troscianko and Martin Stevens. Image calibration and analysis toolbox—a free
626 software suite for objectively measuring reflectance, colour and pattern. *Methods in*
627 *Ecology and Evolution*, 6(11):1320–1331, 2015.

628 Jolyon Troscianko, John Skelhorn, and Martin Stevens. Quantifying camouflage: how to
629 predict detectability from appearance. *BMC evolutionary biology*, 17(1):1–13, 2017.

630 James P. Tumulty, Sara E. Miller, Steven M. Van Belleghem, Hannah I. Weller, Christo-
631 pher M. Jernigan, Sierra Vincent, Regan J. Staudenraus, Andrew W. Legan, Timothy J.
632 Polnaszek, Floria M. K. Uy, Alexander Walton, and Michael J. Sheehan. Evidence for
633 a selective link between cooperation and individual recognition. *bioRxiv*, 2021. doi:
634 10.1101/2021.09.07.459327. URL <https://www.biorxiv.org/content/early/2021/09/08/2021.09.07.459327>.

635

636 M Valcu and J Dale. colorzapper: Color extraction utilities. r package version 1.0, 2014.

637 Jennifer J Valvo, Jose David Aponte, Mitch J Daniel, Kenna Dwinell, Helen Rodd,
638 David Houle, and Kimberly A Hughes. Using delaunay triangulation to sample whole-
639 specimen color from digital images. *Ecology and evolution*, 11(18):12468–12484, 2021.

640 Steven M Van Belleghem, Riccardo Papa, Humberto Ortiz-Zuazaga, Frederik Hendrickx,
641 Chris D Jiggins, W Owen McMillan, and Brian A Counterman. patternize: An r
642 package for quantifying colour pattern variation. *Methods in Ecology and Evolution*, 9
643 (2):390–398, 2018.

644 Steven M Van Belleghem, Paola A Alicea Roman, Heriberto Carbia Gutierrez, Brian A
645 Counterman, and Riccardo Papa. Perfect mimicry between heliconius butterflies is
646 constrained by genetics and development. *Proceedings of the Royal Society B*, 287
647 (1931):20201267, 2020.

648 Cedric P. van den Berg, Jolyon Troscianko, John A. Endler, N. Justin Marshall, and
649 Karen L. Cheney. Quantitative Colour Pattern Analysis (QCPA): A comprehensive

650 framework for the analysis of colour patterns in nature. *Methods in Ecology and Evo-*
651 *lution*, 11(2):316–332, 2020. ISSN 2041210X. doi: 10.1111/2041-210X.13328.

652 François Vuilleumier. Pleistocene speciation in birds living in the high andes. *Nature*,
653 223(5211):1179–1180, 1969.

654 Hannah I Weller and Mark W Westneat. Quantitative color profiling of digital images
655 with earth mover’s distance using the r package colordistance. *PeerJ*, 7:e6398, 2019.

656 Hadley Wickham, Jim Hester, Winston Chang, and Maintainer Jim Hester. Package
657 ‘devtools’. 2021.

658 Canchao Yang, Longwu Wang, Wei Liang, and Anders P Møller. Do common cuckoos
659 (*cuculus canorus*) possess an optimal laying behaviour to match their own egg pheno-
660 type to that of their oriental reed warbler (*acrocephalus orientalis*) hosts? *Biological*
661 *Journal of the Linnean Society*, 117(3):422–427, 2016.

662 Bao Zhou. Image segmentation using slic superpixels and affinity propagation clustering.
663 *Int. J. Sci. Res*, 4(4):1525–1529, 2015.